Sigma J Eng & Nat Sci 38 (2), 2020, 741-756

Sigma Journal of Engineering and Natural Sciences
Sigma Mühendislik ve Fen Bilimleri Dergisi

Research Article

INVESTIGATION OF HEAD AND BED MORTAR REGION EFFECT IN MICRO SCALE MODELLING OF MASONRY WALLS

Muhammet KARATON*[1], Kağan ÇANAKÇI[2]

[1]*Fırat University, Civil Engineering Department, ELAZIG;* ORCID: 0000-0002-1498-4659
[2]*Fırat University, Civil Engineering Department, ELAZIG;* ORCID: 0000-0002-8701-2762

Received: 01.12.2019 Revised: 06.04.2020 Accepted: 04.05.2020

ABSTRACT

In this study, the effectiveness on the micro-model analysis by finite element method of masonry walls of head and bed mortar region is investigated. 3 dimensional fixed smeared crack model is preferred for the nonlinear behavior of mortar and brick regions of the walls. Failure surface of William-Warnke model is used for cracking and crushing calculations. For numerical investigation, experimental results of the Eindhoven walls are selected. The base shear force-top displacement curve and the fracture zones obtained from the experimental results of these walls are used for the comparison of the numerical results. Mortar region in finite element model is discretized two different material as bed and head regions. The effects on the numerical solutions of the two different mortar material are evaluated with regard to different material strength and different shear stress transfer coefficients. The experimental and numerical results are compared in terms of maximum base shear force, threshold displacement values and the fracture zones. According to evidence obtained from numerical solutions, it is observed that closest results to experimental results are obtained for base shear force and threshold displacement. A ratio between tensile and compressive strength of the head and the bed mortar regions are proposed. Values for shear retention factors using in opening and closing cases of the cracking regions where occurred into the two mortar materials, are recommended.
Keywords: Eindhoven walls, micro modelling, fixed smeared crack model, shear retention factors, head and bed mortar regions.

1. INTRODUCTION

Masonry walls have been used for building construction since centuries and are still the preferred as building elements, although the complex behavior of the materials of this structural elements is unknown. Masonry walls are constructed in a concrete or steel frame as filling material or as a support element. Masonry walls are contributed positively to seismic behavior of buildings during an earthquake. Therefore, the behavior of these structural elements needs to be modeled correctly. Different calculation methods was presented for determining the behavior of these structural elements under static and dynamic loads. These calculation methods was categorized into three groups as micro, macro and simplified micro scale analysis [1]. In micro-scale analyzes the correct behavior of the structure is important, and the trajectory of the cracks is more important in the nonlinear behavior of these components. In macro and simplified micro

* Corresponding Author: e-mail: mkaraton@firat.edu.tr, tel: (424) 237 00 00

scale analysis, global behavior of components is important. The nonlinear behavior of each component is not detailed. Although, there is some lack of information in the micro scale approach, crack and damage models have been still preferred for numerical analysis of the masonry walls [4-10] due to the predictions made by this type of analysis are quite reasonable. One of the most widely used models within these models is the Fixed smeared crack model. Adam et al.[4] performed micro-mechanical modeling by a finite element method for a series of laboratory tests on masonry structures. Mortar and brick were modeled as solid material at the finite element model. Nonlinear behavior of the solid domains were modelled by 3 dimensional (3D) smeared crack approach. The interface of these two materials which head and bed joints, was modeled with 3D elasto-plastic interface elements. The results of the non-linear numerical analysis and the experimental results were compared in terms of load-displacement and bending moment-rotation responses. Mohyeddin et al. [5] obtained analyzes of reinforced concrete frames filled with masonry walls using three-dimensional solid finite elements. In order to validate this model, experimental data in the literature were used. Regular masonry walls in the frames were modelled by using head and bed joint elements. Interface elements were used in these joint regions. The solutions were obtained by using ANSYS software. It was observed that the model accurately reflected the effect on the fill frame in-plane and out-of-plane loading cases. Nazir and Dhanasekar [6] used a nonlinear interface element for high adhesive polymer mortared masonry units. Its theory was based on plastic analysis approach. Tests of uniaxial compression, shear and flexural beam of the masonry wall were used for calibrating of the method. Calderon et.al [7] investigated opening effect on the seismic response of the partially grouted masonry walls. Experimental results were compared with numerical analysis of these walls which obtained by using micro modelling technique. Rotating smeared crack model were used for cracking behavior in the brick and mortar units. Interface elements were also used between these masonry units. A good approximation were obtained for displacement ductility, maximum lateral load and failure mode. Petracca et al.[8] presented a novel damage mechanic model for the analysis micro scale of masonry walls. No interface element was use for the numerical solutions. For verification of the model was compared with Eindhoven wall test results and analysis results of discrete micro modeling methods in the literature. D'Altri et al. [9] developed a 3D micro model element in-plane and out-of-plane. The theory of element were based on plastic damage model approach and cohesive interface elements were used between the different masonry units. Numerical results were compared with experimental tests for verifying of the proposed model. Droghas et al. [10] tested small scale masonry walls under the shear loading in-plane in laboratory. Numerical analyzes of these masonry walls were obtained with 3D solid elements and with interface elements between solid domains by using micro modelling approach. Numerical and experimental results were compared in terms of base shear force and, appropriate results were obtained.

In fixed smeared crack model, no effect of material properties of head and bed joints and, of the shear stress transfer coefficient has been investigated until nowadays. Interface element are used for two different domain interaction. Therefore, effect of the joints and the coefficients on these micro model analysis of the masonry walls should be investigated.

In this study, the effectiveness on the micro-model analysis by finite element method of masonry walls of head and bed mortar region is investigated. The nonlinear behavior of mortar and brick regions of the walls are simulated by 3 dimensional fixed smeared crack model. Failure surface of William-Warnke model is used for cracking and crushing calculations. Experimental results of the Eindhoven walls are desired for comparisons of numerical solutions. In numerical analyzes, Solid65 concrete element in Ansys finite element program is selected. The mortar and brick regions are assumed that have different material properties in the finite element model. No-interface element are used for this two different domain. Additionally, mortar is discretized for two different material as bed and head regions. The effects on the numerical solutions of the two different mortar material are assessed with regard to different material strength and different shear stress transfer coefficients. The effects on the numerical solutions of the two different mortar

material are evaluated with regard to different material st rength and different shear stress transfer coefficients. The experimental and numerical results are compared in terms of maximum base shear force, threshold displacement values and the fracture zones. According to evidence obtained from numerical solutions, it is observed that closest results to experimental results are obtained for base shear force and threshold displacement. A ratio between tensile and compressive strength of the head and the bed mortar regions are proposed. Values for shear retention factors using in opening and closing cases of the cracking regions where occurred into the two mortar materials, are recommended.

2. WILLIAM AND WARKNE MODEL

In this study, William and Warnke which a special model of the three parameter model concrete model, is used. The model was developed by William [11]. It describes the collapse surface for concrete in sections subjected to tensile stress under low hydrostatic pressure. Zeinkiewicz and Taylor [12] have demonstrated that this material model can use for brittle materials such as concrete. Concrete collapse surface model of the William-Warnke use effectively in large-scale modeling of masonry structures [1]. This model has a view similar to a cone with a convex cross-section as shown in Fig. 1.a. convex section, symmetrical and smooth structure. Drucker-Prager or von Mises approaches can be identify as a special case of this model since such a cross-section can easily resemble a circle [13]. In this model, the material shows linear elastic behavior when the stress values remaining within the collapse surface. Cracking and crushing behaviors in the material are occurred for the stress values that outside the collapse surface. Cracking in the material are taken into account by the stress softening as seen in Fig. 1.b.

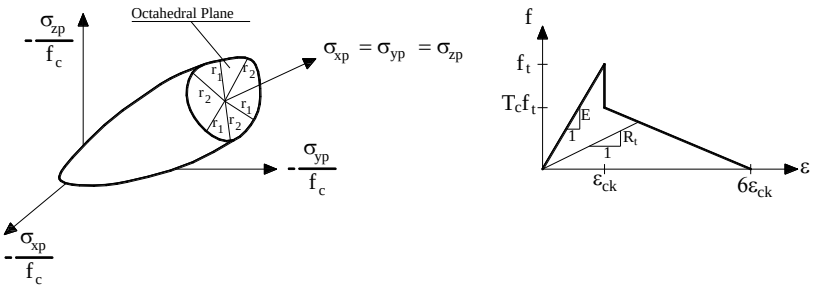

Figure 1. a) collapse surface and b) uniaxial stress-strain relationship for the three-parameter model [13].

3. MICRO MODEL ANALYZES OF JD4, JD6 AND JD7 EINDHOVEN MASONRY WALLS

In this study, nonlinear analyzes of JD4, JD6 and JD7 Eindhoven masonry walls were obtained by micro modeling approach. The dimensions of these walls were 990×1000×100 mm and, were built with 210×52×100 mm bricks and 16 rows of brick-mortar with mortar thickness of 10 mm. There are two rows of steel beams at the top and bottom of the model. In the experimental study, a vertical distributed load applied to the upper beam as a preload and, in the next loading step; a horizontal displacement load applied to the same beam to obtain the bearing strength of the wall. This preload condition was applied as 30, 120 and 210 kN and, the walls for these loading values were called as JD4, JD6 and JD7, respectively [14].

In the micro model of the walls, the material properties for the mortar and the brick, were separately defined. The mortar was also divided into two different materials as bed and head regions (Fig. 2). The connection between the materials was considered as to be rigid. The finite element model were established by 33600 nodes and 21978 three-dimensional solid finite elements. Proposed equalities by Hemant et al.[15] were preferred for elastic material properties of brick and mortar materials. The elasticity modulus of brick material are calculated as,

$$E_b = 300 f_{b,c} \quad \text{(MPa)} \tag{1}$$

in where, $f_{b,c}$ shows the uniaxial compressive strength of the brick. The uniaxial tensile strength of brick material, $f_{b,t}$ is calculated by

$$f_{b,t} = f_{b,c} / 25 \quad \text{(MPa)} \tag{2}$$

Relationship between elasticity modulus (E_m) of mortar and uniaxial compressive strength ($f_{m,c}$) of mortar material is given as,

$$E_m = 200 f_{m,c} \quad \text{(MPa)} \tag{3}$$

The uniaxial tensile strength ($f_{m,t}$) of the mortar is estimated by

$$f_{m,t} = f_{m,c} / 20 \quad \text{(MPa)} \tag{4}$$

Boundary conditions are applied to the bottom surface of the steel beams at the base as fixed in horizontal and vertical directions. To the upper surface of the top steel beam is defined as initial displacement that occurs due to pre loading in only the vertical direction. Ansys software is used for the numerical solutions [13]. In the preloading phase, the weight of the wall and the vertical loads (30, 120 and 210 kN) are applied to the upper beam. At the next loading stage, these loads and displacement values are considered as initial conditions. In the second loading phase, displacement controlled loading are applied at left side of upper steel beam.

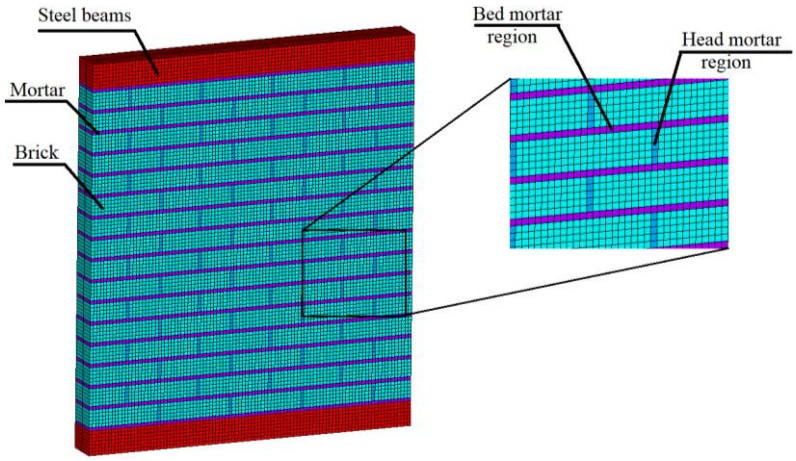

Figure 2. Finite element model and bed/head mortar regions of Eindhoven walls.

3.1. The Effect on Solutions of Material Strength of Head Mortar Region

In this section, effects on the numerical analysis of the JD4, JD6 and JD7 Eindhoven walls of the tensile and compressive strength of head mortar region were investigated. The uniaxial compressive strength of the head mortar region was chosen as 10, 15, 20, 25 and 30 MPa,

respectively. The elasticity modulus values of the mortar was calculated by the Equation (1). The uniaxial tensile strength values of the mortar was taken into account using the coefficient 1/20. The shear stress transfer coefficient was considered as 0.05 and 0.90 for the opening and closing cases of the crack, respectively.

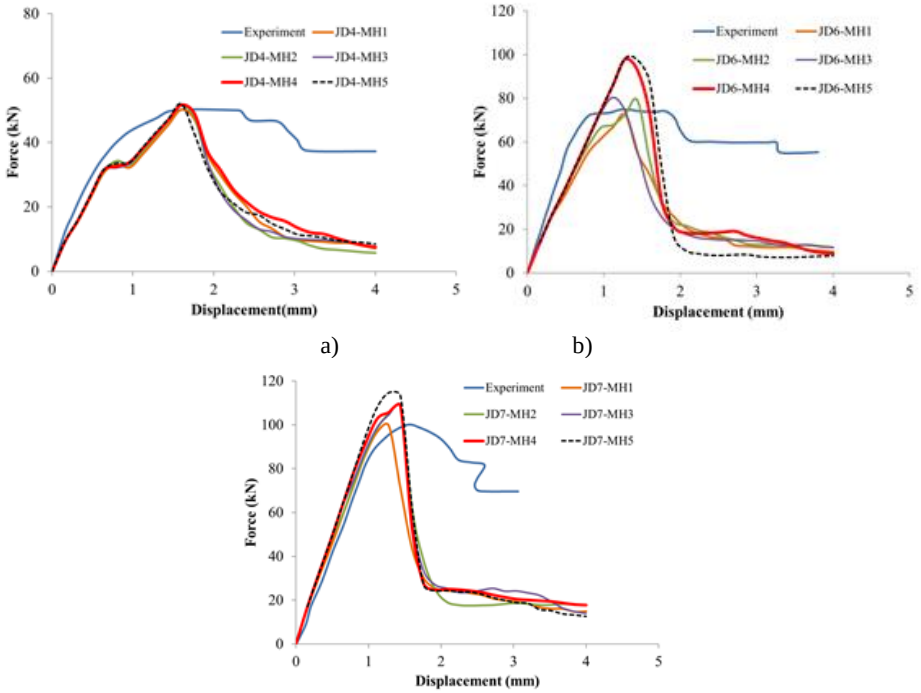

Figure 3. Experimental and numerical force-displacement graphs of a) JD4, b) JD5 and c) JD6 Eindhoven walls for different material strength of the head mortar region.

JD4 walls numerical solutions were called as JD4-MH1, JD4-MH2, JD4-MH3, JD4-MH4 and JD4-MH5 for 10, 15, 20, 25 and 30 MPa of the uniaxial compressive strength of the head region of the mortar, respectively. The maximum base-shear force of the JD4 wall was determined as 50.30 kN from the experimental test result. Base shear force values calculated from numerical analyzes were obtained as 50.21, 51.40, 51.53, 51.64 and 52.02 kN for JD4-MH1, JD4-MH2, JD4-MH3, JD4-MH4 and JD4-MH5, respectively (Fig. 3.a). When comparisons of maximum values of base shear force with the results of the experiment, differences were determined as 0.13%, 2.52%, 2.51%, 2.71% and 3.48%, for the JD4-MH1, JD4-MH2, JD4-MH3, JD4-MH4 and JD4-MH5, respectively. It can be seen that the minimum difference was calculated for JD4-MH1 (Fig.3.a).

The threshold displacement value versus maximum load of the JD4 wall was determined as 1.74 mm from the experimental results. In the numerical analyzes, this displacement value for all numerical solutions of JD4 was calculated as 1.60 mm (Fig. 3.a). This displacement value was compared with experimental result and a difference was found smaller 8.05% than experimental result for all JD4 walls. The minimum differences for base shear force and threshold displacement values were obtained from JD4-MH1 solution.

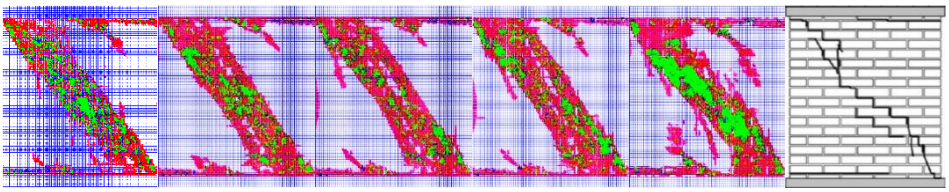

a) JD4-MH1 b) JD4-MH2 c) JD4-MH3 d) JD4-MH4 e) JD4-MH5 f) Experiment

Figure 4. Experimental and numerical cracking zones of JD4 Eindhoven wall for different material strength of head mortar region.

Cracking zones obtained from the experimental and numerical analysis results of the JD4 wall are seen in Fig. 4. Cracking zones of all JD4 walls were plotted at threshold displacement values. In the all solutions, the fracture zones obtained as three regions. First region started from the upper right corner of the JD4 wall and it propagated to the left side in the horizontal direction. Second region started from the bottom left corner of the JD4 wall and it propagated to the right side in the horizontal direction. Additional fracture zone was obtained as diagonal form that propagated from the upper left corner to the bottom right corner.

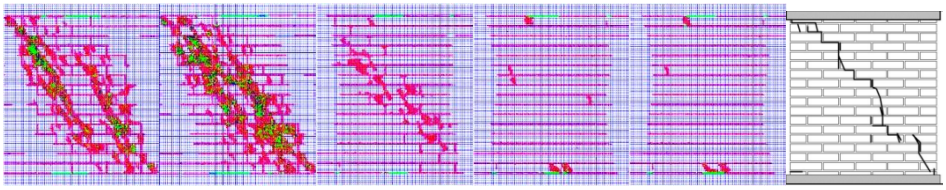

a) JD6-MH1 b) JD6-MH2 c) JD6-MH3 d) JD6-MH4 e) JD6-MH5 f) Experiment

Figure 5. Experimental and numerical cracking zones of JD6 Eindhoven wall for different material strength of head mortar region.

JD6 walls numerical solutions were called as JD6-MH1, JD6-MH2, JD6-MH3, JD6-MH4 and JD6-MH5 for 10, 15, 20, 25 and 30 MPa of the uniaxial compressive strength of the head region of the mortar, respectively. The maximum base-shear force of the JD6 wall was determined as 74.87 kN from the experimental test result. Base shear force values calculated from numerical analyzes were obtained as 72.46, 79.05, 80.41, 97.88 and 98.36 kN for the JD6-MH1, JD6-MH2, JD6-MH3, JD6-MH4 and JD6-MH5, respectively (Fig.3.b). Maximum values of base shear force were compared with the results of the experiment. Differences were calculated as 3.22%, 5.89%, 7.39%, 30.74% and 31.37%, for JD6-MH1, JD6-MH2, JD6-MH3, JD6-MH4 and JD6-MH5, respectively. The minimum difference was observed for JD6-MH1 solution.

The threshold displacement value of the JD6 wall versus maximum base shear force was determined as 1.22 mm from the experimental results. In numerical analyzes, this value was calculated as 1.28, 1.44, 1.12, 1.28 and 1.28 mm for the JD6-MH1, JD6-MH2, JD6-MH3, JD6-MH4 and JD6-MH5, respectively (Fig.3.b). Differences between experimental results and the JD6-MH1, JD6-MH2, JD6-MH3, JD6-MH4, JD6-MH5 solutions were obtained as 4.92%, 18.03%, 8.20%, 4.92% and 4.92%, respectively. The minimum differences for base shear force and threshold displacement values were obtained in JD6-MH1 solution. Cracking zones obtained from the experimental and numerical analysis results of the JD6 wall were shown in Fig.5.

The Cracking zones of all JD6 walls were plotted at threshold displacement values. In the all solutions, the fracture zones obtained as three regions. First region started from the upper right corner of the JD6 wall and it propagated to the left side in the horizontal direction. Second region started from the bottom left corner of the JD6 wall and it propagated to the right side in the

horizontal direction. Additional fracture zone was obtained as diagonal form that propagated from the upper left corner to the bottom right corner for JD6-MH1, JD6-MH2, and JD6-MH3. Furthermore, cracking zones of JD6-MH4 and JD6-MH5 placed in horizontal form.

JD7 walls numerical solutions were called as JD7-MH1, JD7-MH2, JD7-MH3, JD7-MH4 and JD7-MH5 for 10, 15, 20, 25 and 30 MPa of the uniaxial compressive strength of the head region of the mortar, respectively. The maximum base-shear force of the JD7 wall was determined as 100.17 kN from the experimental test result. Base shear force values calculated from numerical analyzes were obtained as 99.63, 108.42, 108.95, 108.57 and 114.63 kN for JD7-MH1, JD7-MH2, JD7-MH3, JD7-MH4 and JD7-MH5, respectively. Maximum value of base shear force was compared with the results of the experiment. Differences for the JD7-MH1, JD7-MH2, JD7-MH3, JD7-MH4, JD7-MH5 solutions were determined as 0.55%, 8.23%, 8.77%, 8.38%, 14.43%, respectively. Minimum difference was calculated for JD7-MH1 (Fig. 3.c).

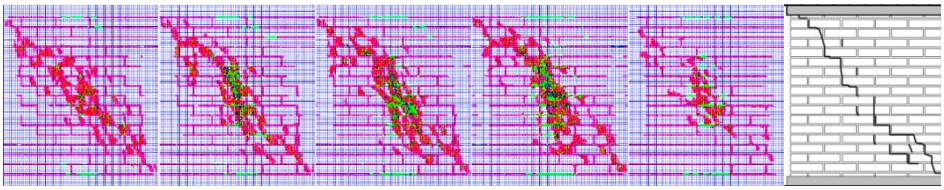

a) JD7-MH1 b) JD7-MH2 c) JD7-MH3 d) JD7-MH4 e) JD7-MH5 f) Experiment

Figure 6. Experimental and numerical cracking zones of JD7 Eindhoven wall for different material strength of head mortar region.

The threshold displacement value of the JD7 wall versus maximum load was obtained as 1.56 mm in the experimental results. This displacement value calculated from the numerical analyzes of the JD7-MH1, JD7-MH2, JD7-MH3, JD7-MH4 and JD7-MH5 was 1.28, 1.44, 1.44, 1.44, 1.28 mm, respectively (Fig.3.c). The differences between experimental results with the JD7-MH1, JD7-MH2, JD7-MH3, JD7-MH4, JD7-MH5 solutions were found as 17.95%, 7.69%, 7.69%, 7.69% and 17.95%, respectively. The minimum differences for base shear force and threshold displacement values were achieved for JD7-MH2 solution.

Cracking zones obtained from the experimental and numerical analysis results of the JD7 wall are shown in Fig.6. Cracking zones of all JD7 walls were plotted at threshold displacement values. In the all numerical solutions, the fracture zones were obtained as three regions. First region started from the upper right corner of the JD7 wall and it propagated to the left side in the horizontal direction. Second region started from the bottom left corner of the JD7 wall and it propagated to the right side in the horizontal direction. Additional fracture zone was occurred as diagonal form that propagated from the upper left corner to the bottom right corner for all JD7 walls. When considered to the comparisons of the cracking regions and maximum value of base shear force, it is assumed that solution of the JD7-MH1 is more appropriate than other solutions.

3.2. The Effect on Solutions of Material Strength of Bed Mortar Region

In this section, the effects on numerical solution of tensile and compressive strength of bed region of the mortar were investigated for JD4, JD6 and JD7 Eindhoven walls. The uniaxial compressive strength of the bed region of the mortar was chosen as 10, 15, 20, 25 and 30 MPa respectively. The elasticity modulus values of the mortar were calculated by the Equation (3). The uniaxial tensile strength values of the mortar were taken into account using a scale 1/20. The shear stress transfer coefficient was considered as 0.05 and 0.90 for the opening or closing states of the crack, respectively.

JD4 walls numerical solutions were called as JD4-MB1, JD4-MB2, JD4-MB3, JD4-MB4 and JD4-MB5 for 10, 15, 20, 25 and 30 MPa of the uniaxial compressive strength of the bed region of the mortar, respectively. Base shear force values calculated from numerical analyzes were obtained as 50.21, 54.46, 58.56, 54.37 and 57.88 kN for JD4-MB1, JD4-MB2, JD4-MB3, JD4-MB4 and JD4-MB5, respectively. When maximum value of base shear force was compared with the results of the experiment, differences were determined as 0.13%, 8.34%, 16.48%, 8.16% and 15.13% for the JD4-MB1, JD4-MB2, JD4-MB3, JD4-MB4 and JD4-MB5, respectively.

The threshold displacement value determined from the JD4-MB1, JD4-MB2, JD4-MB3, JD4-MB4 and JD4-MB5 solutions was calculated as 1.60, 1.60, 1.60, 1.44, 1.44 mm, respectively (Fig. 7.a). Differences between experimental results with the JD4-MB1, JD4-MB2, JD4-MB3, JD4-MB4 and JD4-MB5 solutions were showed as 8.05%, 8.05%, 8.05%, 17.24%, 17.24%, respectively. The minimum differences for base shear force and threshold displacement values was obtained from JD4-MB1 solution (Fig.7.a).

Cracking zones obtained from the experimental and numerical analysis results of the JD4 wall were shown in Fig.8. Cracking zones of all JD4 walls were plotted at threshold displacement values. In the all solutions, the fracture zones were obtained as three regions as similar to JD4 solutions in previous section.

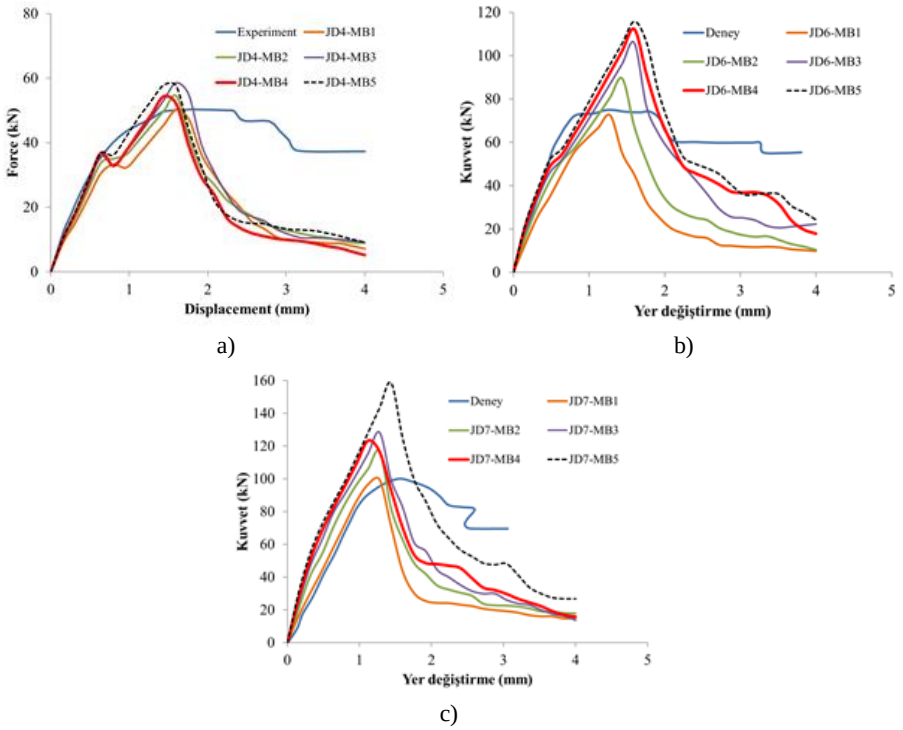

Figure 7. Experimental and numerical force-displacement graphs of a) JD4, b) JD6 and c) JD7 Eindhoven walls for different material strength of the bed mortar region.

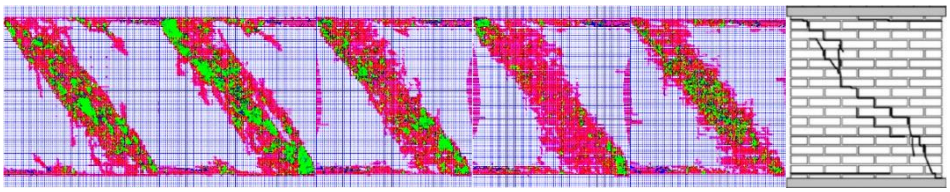

a) JD4-MB1 b) JD4-MB2 c) JD4-MB3 d) JD4-MB4 e) JD4-MB5 f) Experimental

Figure 8. Experimental and numerical cracking zones of JD4 Eindhoven wall for different material strength of bed mortar region.

JD6 walls numerical solutions were called as JD6-MB1, JD6-MB2, JD6-MB3, JD6-MB4 and JD6-MB5 for 10, 15, 20, 25 and 30 MPa of the uniaxial compressive strength of the bed region of the mortar, respectively. Base shear force values calculated from numerical analyzes were obtained as 72.46, 89.05, 105.89, 112.16 and 115.85 kN for the JD6-MB1, JD6-MB2, JD6-MB3, JD6-MB4 and JD6-MB5, respectively (Fig.7.b). Maximum values of base shear force were compared with the results of the experiment. Differences were calculated as 3.22%, 19.48%, 41.22%, 49.80% and 54.73%, for the JD6-MB1, JD6-MB2, JD6-MB3, JD6-MB4 and JD6-MB5, respectively. The minimum difference is shown for JD6-MB1 solution.

The threshold displacement value of the JD6 was 1.22 mm. In numerical analyzes, this value was calculated as 1.28, 1.44, 1.60, 1.60 and 1.60 mm for the JD6-MB1, JD6-MB2, JD6-MB3, JD6-MB4 and JD6-MB5, respectively (Fig.7.b). Differences between experimental results and the JD6-MB1, JD6-MB2, JD6-MB3, JD6-MB4 and JD6-MB5 solutions were obtained as 4.92%, 18.03%, 31.15%, 31.15% and 31.15%, respectively. The minimum differences for base shear force and threshold displacement values were obtained from JD6-MB1 solution. Cracking zones obtained from the experimental and numerical analysis results of the JD6 wall were shown in Fig.9.

The Cracking zones of all JD6 walls were plotted at threshold displacement values. In the all numerical solutions, the fracture zones were obtained as three regions. In the all solutions, the fracture zones were obtained as three regions as similar to JD6 solutions in previous section.

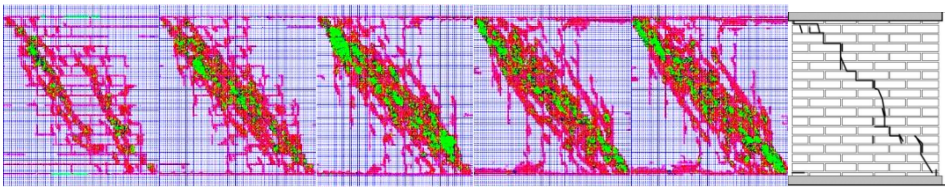

a) JD6-MB1 b) JD6-MB2 c) JD6-MB3 d) JD6-MB4 e) JD6-MB5 f) Experiment

Figure 9. Experimental and numerical cracking zones of JD6 Eindhoven wall for different material strength of bed mortar region.

JD7 walls numerical solutions were called as JD7-MB1, JD7-MB2, JD7-MB3, JD7-MB4 and JD7-MB5 for 10, 15, 20, 25 and 30 MPa of the uniaxial compressive strength of the bed region of the mortar, respectively. Base shear force values calculated from numerical analyzes were obtained as 99.63, 116.63, 128.41, 123.46 and 158.68 kN for JD7-MB1, JD7-MB2, JD7-MB3, JD7-MB4 and JD7-MB5, respectively. When maximum value of base shear force was compared with the results of the experiment, differences were determined as 0.55%, 16.46%, 28.19%, 23.25% and 58.41% for the JD7-MB1, JD7-MB2, JD7-MB3, JD7-MB4 and JD7-MB5 solutions, respectively. Minimum difference was calculated for JD7-MB1 (Fig. 7.c).

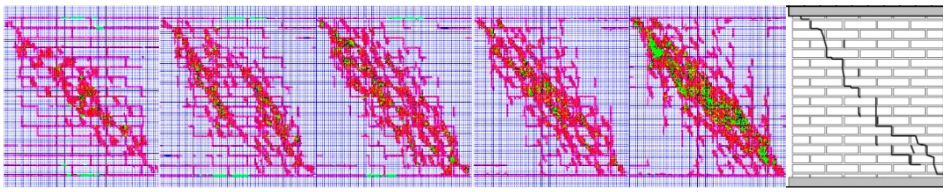

a) JD7-MB1 b) JD7-MB2 c) JD7-MB3 d) JD7-MB4 e) JD7-MB5 f) Experiment

Figure 10. Experimental and numerical cracking zones of JD7 Eindhoven wall for different material strength of bed mortar region.

The threshold displacement value for the JD7-MB1, JD7-MB2, JD7-MB3, JD7-MB4 and JD7-MB5 the numerical analyzes was calculated as 1.28, 1.28, 1.28, 1.12 and 1.44 mm, respectively (Fig.7.c). The differences for the displacement value between experimental results with JD7-MB1, JD7-MB2, JD7-MB3, JD7-MB4 and JD7-MB5 solutions were calculated as 17.95%, 17.95%, 17.95%, 28.21% and 7.69% respectively. The minimum differences for base shear force and threshold displacement values were obtained from JD7-MB1 solution. Cracking zones obtained from the experimental and numerical analysis results of the JD7 wall are shown in Fig.10. Cracking zones of all JD7 walls were plotted at threshold displacement values. In the all solutions, the fracture zones were obtained as three regions as similar to JD7 solutions in previous section.

3.3. Effect on Solution of Shear Transfer Coefficients of the Head Mortar Material

In this section, the effects on the numerical solutions of the Eindhoven walls of the shear transfer coefficient in the opening case, β_t of the head region of the mortar material were investigated. The shear transfer coefficient in the closing case of this region that β_c , was taken as 0.90 [4,5]. β_t coefficient in the numerical solutions was changed as 0.05, 0.1, 0.2, 0.3, 0.4. β_c and β_t coefficients for the head regions and the brick regions in all solutions were taken into account as 0.90 and 0.05, respectively.

Numerical solutions of JD4 walls were called as JD4-MHBT1, JD4-MHBT2, JD4-MHBT3, JD4-MHBT4 and JD4-MHBT5 for 0.05, 0.1, 0.2, 0.3 and 0.4 of β_t coefficient, respectively. Base shear force values calculated from JD4-MHBT1, JD4-MHBT2, JD4-MHBT3, JD4-MHBT4 and JD4-MHBT5 numerical analyzes were 50.21, 50.49, 50.77, 46.21 and 46.33 kN, respectively. When maximum value of base shear force was compared with the results of the experiment, differences for the JD4-MHBT1, JD4-MHBT2, JD4-MHBT3, JD4-MHBT4 and JD4-MHBT5 were determined as 0.13%, 0.44%, 1.00%, 8.08% and 7.85%, respectively.

The threshold displacement value of the JD4 wall was 1.74 mm. In numerical analyzes, this displacement value was calculated as 1.60, 1.60, 1.60, 1.44, 1.44 mm for the JD4-MHBT1, JD4-MHBT2, JD4-MHBT3, JD4-MHBT4 and JD4-MHBT5, respectively (Fig. 11.a). Differences between experimental results with the JD4-MHBT1, JD4-MHBT2, JD4-MHBT3, JD4-MHBT4 and JD4-MHBT5 solutions were determined as 8.05%, 8.05%, 8.05%, 17.24%, 17.24%, respectively. The minimum differences for base shear force and threshold displacement values was obtained from JD4-MB1 solution (Fig. 11.a). Cracking zones obtained from the experimental and numerical analysis results of the JD4 wall were shown in Fig.12. Cracking zones of all JD4 walls were plotted at threshold displacement values. In the all solutions, the fracture zones were obtained as three regions as similar to JD4 solutions in previous section.

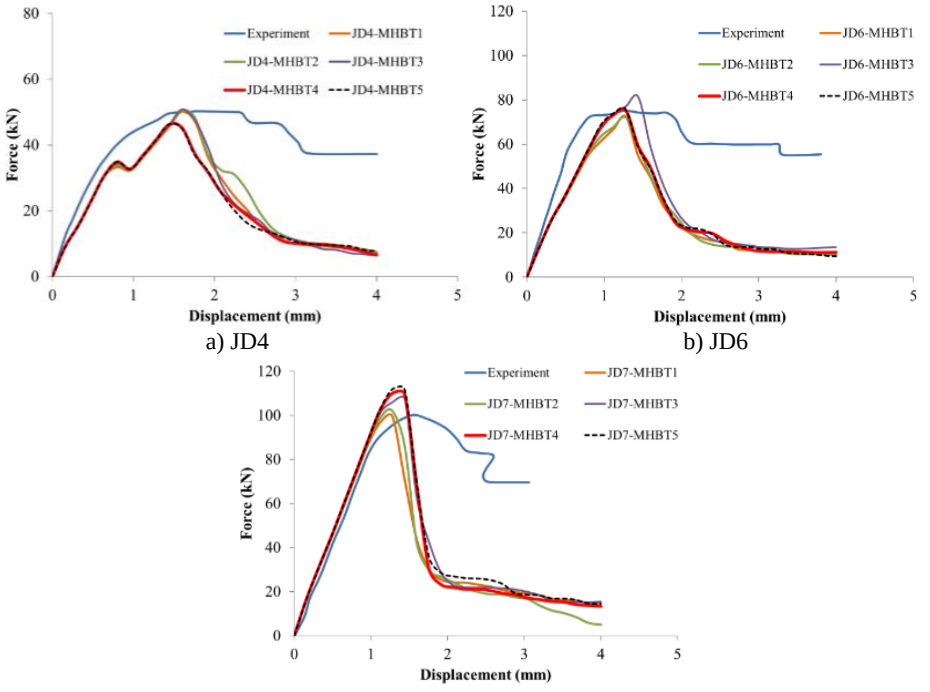

a) JD4 b) JD6

c) JD7

Figure 11. Experimental and numerical force-displacement graphs for different β_t values of the head mortar region of the Eindhoven walls.

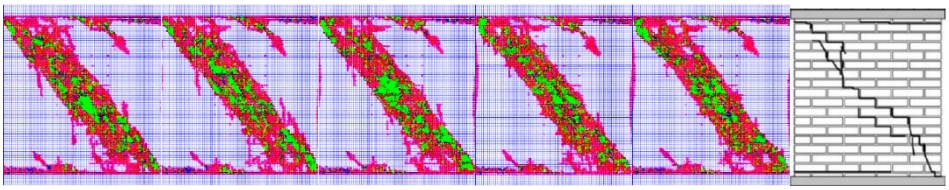

a) JD4-MHBT1 b) JD4-MHBT2 c) JD4-MHBT3 d) JD4-MHBT4 e) JD4-MHBT5 f) Experiment

Figure 12. Experimental and numerical cracking zones for different β_t values of the head mortar region of the JD4 Eindhoven wall.

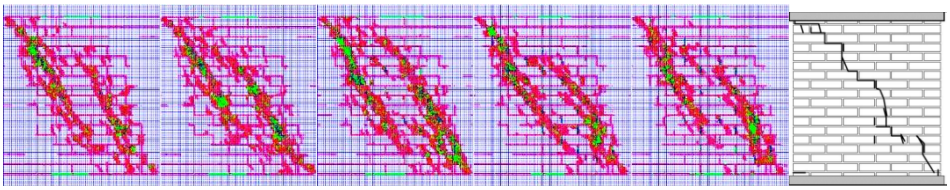

a) JD6- MHBT1 b) JD6-MHBT2 c) JD6-MHBT3 d) JD6-MHBT4 e) JD6-MHBT5 f) Experiment

Figure 13. Experimental and numerical cracking zones for different β_t values of the head mortar region of the JD6 Eindhoven wall.

JD6 walls numerical solutions were called as JD6-MHBT1, JD6-MHBT2, JD6-MHBT3, JD6-MHBT4 and JD6-MHBT5 for 0.05, 0.1, 0.2, 0.3 and 0.4 values of β_t coefficient, respectively. Base shear force values calculated from the JD6-MHBT1, JD6-MHBT2, JD6-MHBT3, JD6-MHBT4 and JD6-MHBT5 numerical analyzes were 72.46, 72.07, 81.35, 75.14 and 75.54 kN, respectively (Fig. 11.b). Differences between experimental results and the JD6-MHBT1, JD6-MHBT2, JD6-MHBT3, JD6-MHBT4 and JD6-MHBT5 solutions were determined as 3.22%, 3.74%, 8.65%, 0.38% and 0.90%, respectively.

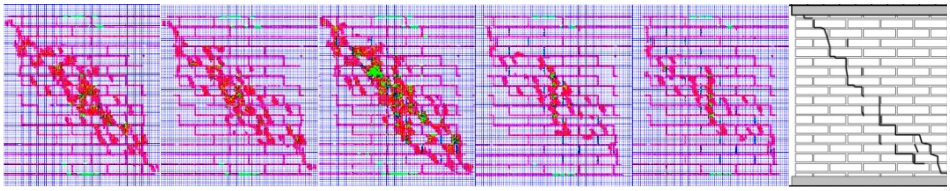

a) JD7-MHBT1 b) JD7-MHBT c) JD7-MHBT3 d) JD7-MHBT4e) JD7-MHBT5 f) Experiment

Figure 14. Experimental and numerical cracking zones for different β_t values of the head mortar region of the JD7 Eindhoven wall.

The threshold displacement values was calculated as 1.28, 1.28, 1.44, 1.28, 1.28 mm for the JD6-MHBT1, JD6-MHBT2, JD6-MHBT3, JD6-MHBT4 and JD6-MHBT5, respectively (Fig.11.b). Differences between experimental results and the JD6-MHBT1, JD6-MHBT2, JD6-MHBT3, JD6-MHBT4, JD6-MHBT5 solutions were obtained as 4.92%, 4.92%, 18.03%, 4.92%, 4.92%, respectively. The minimum differences with regard to base shear force and threshold displacement values were obtained from JD6-MHBT1 solution. The Cracking zones of all JD6 walls were plotted at threshold displacement values. In the all solutions, the fracture zones were obtained as three regions as similar to JD6 solutions in previous section (Fig.13).

JD7 walls numerical solutions were called as JD7-MHBT1, JD7-MHBT2, JD7-MHBT3, JD7-MHBT4 and JD7-MHBT5 for 0.05, 0.1, 0.2, 0.3 and 0.4 of β_t coefficient, respectively. Base shear force values calculated from numerical analyzes were obtained as 99.63, 101.99, 107.63, 110.00 and 111.95 kN for JD7-MHBT1, JD7-MHBT2, JD7-MHBT3, JD7-MHBT4 and JD7-MHBT5, respectively (Fig.11.c). Maximum value of base shear force was compared with the results of the experiment. The differences were determined as 0.55%, 1.82%, 7.44%, 9.81% and 11.76% for the JD7-MHBT1, JD7-MHBT2, JD7-MHBT3, JD7-MHBT4 and JD7-MHBT5 solutions, respectively.

The threshold displacement values were determined as 1.28, 1.28, 1.44, 1.28 and 1.28 mm for numerical analyzes of the JD7-MHBT1, JD7-MHBT2, JD7-MHBT3, JD7-MHBT4 and JD7-MHBT5 walls, respectively (Fig.11.c). The differences between experimental results with the JD7-MHBT1, JD7-MHBT2, JD7-MHBT3, JD7-MHBT4 and JD7-MHBT5 solutions were calculated as 17.95%, 17.95%, 7.69%, 17.95% and 17.95%, respectively. The minimum differences for base shear force and threshold displacement values were obtained in JD7-MHBT3 solution.

Cracking zones of all JD7 walls were plotted at threshold displacement values. In the all solutions, the fracture zones were obtained as three regions as similar to JD7 solutions in previous section (Fig.14).

3.4. Effect on Solution of Shear Transfer Coefficient of the Bed Mortar Material

In this section, the effects on the numerical solutions of the Eindhoven walls of the shear transfer coefficient in the opening case, β_t of the bed region of the mortar material were

investigated. The shear transfer coefficient in the closing case, β_c was taken as 0.90. β_t coefficient in the numerical solutions was changed as 0.05, 0.1, 0.2, 0.3, 0.4. β_c and β_t coefficients for the bed regions. The brick regions in all solutions were taken into account as 0.90 and 0.05, respectively.

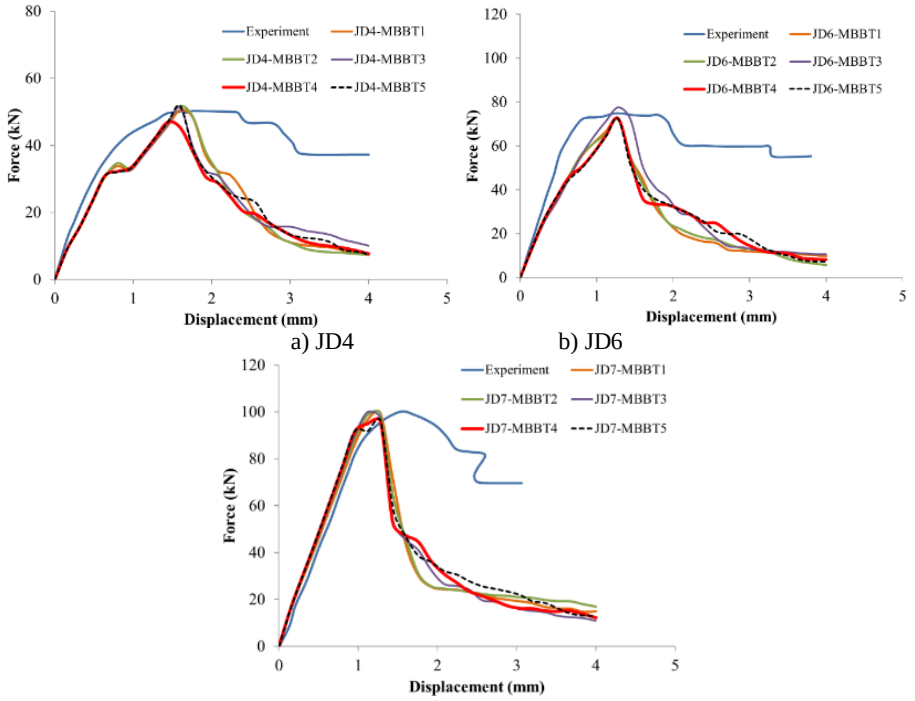

Figure 15. Experimental and numerical force-displacement graphs for different β_t values of the bed mortar region of the Eindhoven walls.

JD4 walls numerical solutions were called as JD4-MBBT1, JD4-MBBT2, JD4-MBBT3, JD4-MBBT4 and JD4-MBBT5 for 0.05, 0.1, 0.2, 0.3 and 0.4 of β_t coefficient, respectively. The maximum base-shear force of the JD4 wall was 50.30 kN from the experimental test result. Base shear force values calculated from numerical analyzes were obtained as 50.49, 51.85, 51.15, 46.88 and 51.81 kN for JD4-MBBT1, JD4-MBBT2, JD4-MBBT3, JD4-MBBT4 and JD4-MBBT5, respectively. Maximum value of base shear force was compared with the results of the experiment. Differences were determined as 0.44%, 3.15%, 1.75%, 6.74% and 3.06% for the JD4-MBBT1, JD4-MBBT2, JD4-MBBT3, JD4-MBBT4 and JD4-MBBT5, respectively.

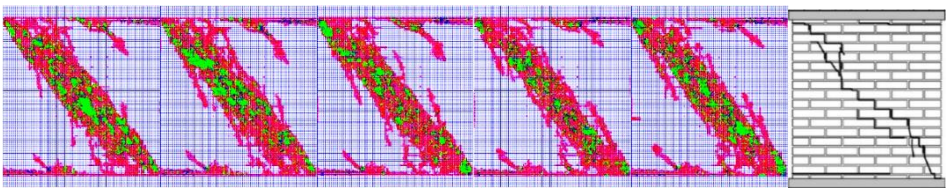

a) JD4-MBBT1 b) JD4-MBBT2 c) JD4-MBBT3 d) JD4-MBBT4 e) JD4-MBBT5 f) Experiment

Figure 16. Experimental and numerical cracking zones for different β_t values of the bed mortar region of the JD4 Eindhoven wall.

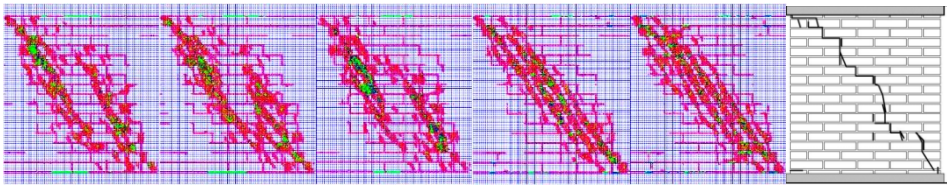

a) JD6-MBBT1 b) JD6-MBBT2 c) JD6-MBBT3 d) JD6-MBBT4 e) JD6-MBBT5 f) Experiment

Figure 17. Experimental and numerical cracking zones for different β_t values of the bed mortar region of the JD6 Eindhoven wall.

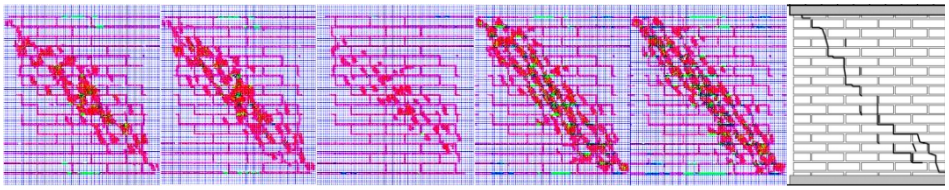

a) JD7-MBBT1 b) JD7-MBBT2 c) JD7-MBBT d) JD7-MBBT4 e) JD7-MBBT5 f) Experiment

Figure 18. Experimental and numerical cracking zones for different β_t values of the bed mortar region of the JD7 Eindhoven wall.

The threshold displacement value of the JD4 wall was 1.74 mm. In numerical analyzes, the displacement value was calculated as 1.60, 1.60, 1.60, 1.44, 1.44 mm for the JD4-MBBT1, JD4-MBBT2, JD4-MBBT3, JD4-MBBT4 and JD4-MBBT5, respectively (Fig.15.a). Differences between experimental results with the JD4-MBBT1, JD4-MBBT2, JD4-MBBT3, JD4-MBBT4 and JD4-MBBT5 solutions were determined as 8.05%, 8.05%, 8.05%, 17.24%, 17.24%, respectively. The minimum differences for base shear force and threshold displacement values were obtained from JD4-MBBT1 solution (Fig.15.a). In the all solutions, the fracture zones were obtained as three regions as similar to JD4 solutions in previous section (Fig.16).

JD6 walls numerical solutions were called as JD6-MBBT1, JD6-MBBT2, JD6-MBBT3, JD6-MBBT4 and JD6-MBBT5 for 0.05, 0.1, 0.2, 0.3 and 0.4 of β_t coefficient, respectively. Base shear force values calculated from numerical analyzes of JD6-MBBT1, JD6-MBBT2, JD6-MBBT3, JD6-MBBT4 and JD6-MBBT5 were 72.46, 72.13, 77.58, 72.51 and 72.34 kN, respectively. Maximum value of base shear force was compared with the results of the experiment. Differences for the JD6-MBBT1, JD6-MBBT2, JD6-MBBT3, JD6-MBBT4 and JD6-MBBT5 were determined as 3.22%, 3.66%, 3.61%, 3.15% and 3.38%, respectively. The minimum difference was calculated for JD6-MBBT4 (Fig. 15.b).

The threshold displacement values were calculated as 1.28 mm for the JD6-MBBT1, JD6-MBBT2, JD6-MBBT3, JD6-MBBT4 and JD6-MBBT5 (Fig. 15.b). Differences between experimental results and the numerical were determined as 4.92% in the all solutions (Fig.15.b). In the all solutions, the fracture zones were obtained as three regions as similar to JD6 solutions in previous section (Fig.17).

Numerical solutions of the JD7 walls were called as JD7-MBBT1, JD7-MBBT2, JD7-MBBT3, JD7-MBBT4 and JD7-MBBT5 for 0.05, 0.1, 0.2, 0.3 and 0.4 of β_t coefficient, respectively. Base shear force values calculated from numerical analyzes were obtained as 99.62, 99.20, 100.06, 96.18 and 96.34 kN for JD7-MBBT1, JD7-MBBT2, JD7-MBBT3, JD7-MBBT4 and JD7-MBBT5, respectively. Maximum value of base shear force was compared with the results of the experiment. Differences for the JD7-MBBT1, JD7-MBBT2, JD7-MBBT3, JD7-MBBT4 and JD7-MBBT5 were determined as 0.55%, 0.97%, 0.12%, 3.98% and 3.82%, respectively.

The threshold displacement values for the JD7-MBBT1, JD7-MBBT2, JD7-MBBT3, JD7-MBBT4 and JD7-MBBT5 were calculated as 1.28, 1.28, 1.12, 1.28 and 1.28 mm, respectively (Fig.15.c). Differences between experimental results with the JD7-MBBT1, JD7-MBBT2, JD7-MBBT3, JD7-MBBT4 and JD7-MBBT5 solutions were determined as 17.95%, 17.95%, 28.21%, 17.95% and 17.95%, respectively. The minimum differences for base shear force and threshold displacement values were obtained from JD7-MBBT1 solution (Fig.15.c). In the all solutions, the fracture zones were obtained as three regions as similar to JD7 solutions in previous section (Fig.18).

4. CONCLUSIONS

In this study, the effectiveness on the micro-model analysis by finite element method of masonry walls of head and bed mortar region is investigated. The nonlinear behavior of mortar and brick regions of the walls are simulated by 3 dimensional fixed smeared crack model. Failure surface of William-Warnke model is used for cracking and crushing calculations. In the cracking model, "shear stress transfer" coefficients are defined for the transfer of shear stresses to the other surface after cracking case. The coefficient for opening and closing cases of a cracking zone is called as β_t and β_c, respectively. Experimental results of the Eindhoven walls are preferred for comparisons of numerical solutions. In numerical analyzes, Solid65 concrete element in Ansys finite element program is chosen. The mortar and brick regions are assumed that have different material properties in the finite element model. No-interface element are used for this two different domain. Additionally, mortar is discretized for two different material as bed and head regions. The effects on the numerical solutions of the two different mortar material are evaluated with regard to different material strength and different shear stress transfer coefficients. The experimental and numerical results are compared in terms of maximum base shear force, threshold displacement values and the fracture zones. The results from obtained the numerical solutions are given below;

- In the numerical analysis with micro model of this type masonry walls, β_t and β_c coefficients of the brick and mortar can be chose as 0.05 and 0.90, respectively.
- The uniaxial compressive strength value of the head mortar and the bed mortar region is equal. Tensile strength of the two regions can be calculated by 1/20 of the compressive strength.
- No interface elements are used in all numerical analysis, maximum difference between experimental and numerical results with respect to the base shear force is obtained under 3.5%. Thus, in numerical analysis by using the micro modelling of the masonry walls, simpler finite element model can be established.
- Maximum difference between experimental and numerical results with respect to the threshold displacement is calculated under 18%.

- In the all numerical analysis results, the fracture zones are obtained in the form of two zones in the horizontal direction that propagating to starting from the upper right corner of the walls to left side and propagating to starting from the bottom left corner of the walls to right side. An additional fracture zone is observed in the diagonal direction and it is propagated wider area.

REFERENCES

[1] Karaton M., Aksoy, H.S., Sayın, E. and Calayır, Y., (2017) Nonlinear seismic performance of a 12th century historical masonry bridge under different earthquake levels, *Engineering Failure Analysis* 79, 408-421.

[2] Chaimoon, K., Attard, M.M., (2007), "Modeling of unreinforced masonry walls under shear and compression", *Engineering Structures*, 29, 2056-2068.

[3] Caporale, A., Parisi, F., Asprone, D., Luciano, R., Prota, A., (2013), "Micromechanical analysis of adobe masonry as two-component composite: Influence of bond and loading schemes", *Composite Structures*, 112, 254–263.

[4] Adam, J. M., Brencich A., Hughes, T.G. and Tony Jefferson, T., (2010) Micromodelling of eccentrically loaded brickwork: Study of masonry wallettes", *Engineering Structures* 32(5), 1244-1251.

[5] Mohyeddin, A., Goldsworthy, H.M. and Gad, E.F., (2013) FE modelling of RC frames with masonry infill panels under in-plane and out-of-plane loading, *Engineering Structures* 51, 73-87.

[6] Nazir, S., and Dhanasekar, M., (2014), "A non-linear interface element model for thin layer high adhesive mortared masonry", *Computers and Structures* 144, 23-39.

[7] Calderón, S., Sandoval, C. and Arnau O., (2017) Shear response of partially-grouted reinforced masonry walls with a central opening: Testing and detailed micro-modelling, *Material and Design* 118, 122-137.

[8] Petracca, M., Pelà, L., Rossi. R., Zaghi, S., Camata, G. and Spacone, E., (2017) Micro-scale continuous and discrete numerical models for nonlinear analysis of masonry shear walls", *Construction and Building Material*, 149, 296-314.

[9] D'Altri, A.M., Miranda, S., Castellazzi, G. and Sarhosis V., (2018) A 3D detailed micro-model for the in-plane and out-of-plane numerical analysis of masonry panels, *Computers and Structures* 206, 18–30.

[10] Drougkas, A., Roca, P. and Molins, C., (2019) Experimental analysis and detailed micro-modeling of masonry walls subjected to in-plane shear, *Engineering Failure Analysis* 95, 82-95.

[11] William K.J. and Warnke., (1975) Constitutive Model for the Tri-axial Behaviour of Concrete, *Proceeding of the International Association for Bridge and Structural Engineering*, January, Bergamo, Italy.

[12] Zeinkiewicz, O. C. and Taylor, R. L., (1991) Finite Element Method: Solid and Fluid Mechanics Dynamics and Non-Linearity, 4th Edition. *McGraw-Hill*, New York, NY, USA.

[13] Swanson Analysis System, (2015), *Ansys Version 16*.

[14] Vermeltfoort, A.Th. and Raijmakers, T.M.J., (1993) Deformation Controlled Tests in Masonry Shear Walls, Part 2 (in dutch), Report TUE/BKO/93.08. *Eindhoven University of Technology*, Eindhoven, Netherlands.

[15] Hemant, B. K., Durgesh, C.R., Sudnir K. J., (2007), "Stress-Strain Characteristics of Clay Brick Masonry under Uniaxial Compression", *Journal of Materials in Civil Engineering* 19(9), 728-739.